AD-A189 197 NON-LINEAR MATERIALS (TAS)(U) GEO-CENTERS INC NEWTON CENTRE MA R AUYEUNG 29 JAN 88 GC-TR-88-1716 1/1
N00014-86-C-2326

UNCLASSIFIED F/G 7/2 NL

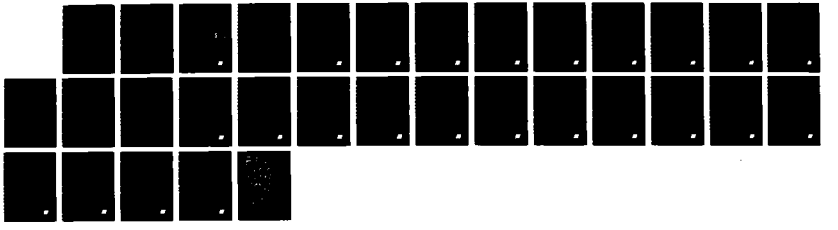

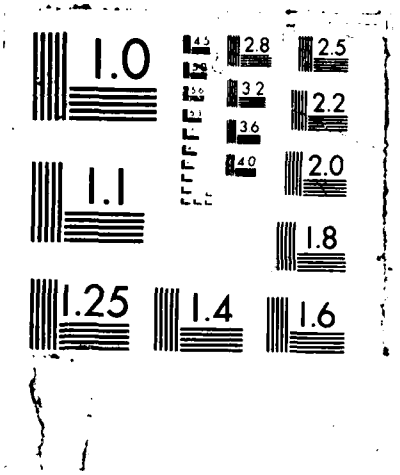
1.0
1.1
1.25
1.4
1.6
1.8
2.0
2.2
2.5
2.8
3.2
3.6
4.0

GC-TR-88-1Z16

AD-A189 197

NON-LINEAR MATERIALS (TAS)

(4)

GC-TR-88-1716

NON-LINEAR MATERIALS (TAS)

PREPARED FOR
NAVAL RESEARCH LABORATORY
4555 OVERLOOK DRIVE, S.W.
WASHINGTON, D.C. 20375-5000
UNDER CONTRACT N00014-86-C-2326

PREPARED BY
GEO-CENTERS, INC.
7 WELLS AVENUE
NEWTON CENTRE, MA 02159

JANUARY 1988

GEO-CENTERS, INC.

UNCLASSIFIED
SECURITY CLASSIFICATION OF THIS PAGE

REPORT DOCUMENTATION PAGE

1a. REPORT SECURITY CLASSIFICATION UNCLASSIFIED	1b. RESTRICTIVE MARKINGS
2a. SECURITY CLASSIFICATION AUTHORITY	3 DISTRIBUTION / AVAILABILITY OF REPORT Approved for public release. Distribution unlimited.
2b. DECLASSIFICATION / DOWNGRADING SCHEDULE	
4. PERFORMING ORGANIZATION REPORT NUMBER(S) GC-TR-88-1716	5. MONITORING ORGANIZATION REPORT NUMBER(S)
6a. NAME OF PERFORMING ORGANIZATION GEO-CENTERS, INC. 6b OFFICE SYMBOL (If applicable)	7a. NAME OF MONITORING ORGANIZATION
6c. ADDRESS (City, State, and ZIP Code) 7 Wells Avenue Newton Centre, MA 02159	7b. ADDRESS (City, State, and ZIP Code)
8a. NAME OF FUNDING / SPONSORING ORGANIZATION Naval Research Laboratory 8b. OFFICE SYMBOL (If applicable) Code 6540	9. PROCUREMENT INSTRUMENT IDENTIFICATION NUMBER
8c. ADDRESS (City, State, and ZIP Code) 4555 Overlook Avenue, S.W. Washington, DC 20375-5000	10. SOURCE OF FUNDING NUMBERS PROGRAM ELEMENT NO. / PROJECT NO. / TASK NO. / WORK UNIT ACCESSION NO

11. TITLE (Include Security Classification)
"Non-Linear Materials (TAS)" - Unclassified

12. PERSONAL AUTHOR(S)
R. Auyeung

13a. TYPE OF REPORT	13b. TIME COVERED	14. DATE OF REPORT (Year, Month, Day)	15 PAGE COUNT
FINAL	FROM 5/86 TO 11/87	1988/January/29	29

16. SUPPLEMENTARY NOTATION

17. COSATI CODES			18. SUBJECT TERMS (Continue on reverse if necessary and identify by block number)
FIELD	GROUP	SUB-GROUP	Frequency Conversion, Tunable Laser Sources, Non-Linear Materials, Thallium Arsenide

19. ABSTRACT (Continue on reverse if necessary and identify by block number)

This report describes the investigation of frequency conversion techniques using the non-linear crystalline material thallium arsenide (TAS). The procedures for the successful generation of frequencies through the fifth harmonic are described, as well as a discussion of optimization of laser output at each frequency.

20 DISTRIBUTION / AVAILABILITY OF ABSTRACT ☒ UNCLASSIFIED/UNLIMITED ☐ SAME AS RPT ☐ DTIC USERS	21 ABSTRACT SECURITY CLASSIFICATION UNCLASSIFIED
22a NAME OF RESPONSIBLE INDIVIDUAL Dr. Barry Feldman	22b TELEPHONE (Include Area Code) 202-767-2028 22c OFFICE SYMBOL Code 6540

DD FORM 1473, 84 MAR 83 APR edition may be used until exhausted
All other editions are obsolete

SECURITY CLASSIFICATION OF THIS PAGE
UNCLASSIFIED

TABLE OF CONTENTS

LIST OF FIGURES

LIST OF FIGURES (Cont'd.)

LIST OF TABLES

I. Introduction.

The U.S. Navy has numerous applications for high power optical sources over the entire infrared spectrum. Among these applications are communications, power transmission, and countermeasures. The CO_2 laser has long been recognized as the standard for high powers at long infrared wavelengths (10.6 μm). A quantum leap in technological capability would result if this high power source could be rendered tunable over specific spectral regions of interest.

This report describes our investigation of frequency conversion techniques using the non-linear crystalline material thallium arsenide (TAS) and other materials to generate harmonics of the CO_2 laser output. We have successfully optimized the laser output for frequency conversion, and have generated frequencies through the fifth harmonic. These results demonstrate that TAS can considerably extend the wavelength range of the CO_2 laser and is a promising candidate for a powerful and tunable source of infrared radiation.

We are also reporting on our work in a related effort investigating the kinetics and potential of the Argon/Xenon laser, using different pumping techniques. Operating on the 5d-6p Xe transitions, we have used electron beam, electron beam sustained discharge, and x-ray preionized discharge pumping methods to evaluate the efficiency and other operating characteristics of this experimental laser system.

II. Non-Linear Materials (TAS).

1. Background.

There exists a need for a powerful and tunable coherent radiation source in the near- to mid-infrared region. Radiation in this region has been generated by direct sources such as HBr, DF, HF, CO and CO_2 lasers and by indirect sources from non-linear materials such as $AgGaSe_2$ and $CdGeAs_2$. Frequency conversion in non-linear materials is an attractive method of generating new IR sources since it can dramatically extend the wavelength coverage of an existing laser and offer the potential for a compact all-solid-state laser system.

The CO_2 laser is an powerful and tunable source of mid-infrared radiation and as a result, has been the focus of the development of new non-linear infrared materials. Most of these materials have met with limited success. Tellurium has the highest non-linear coefficient known but suffers from two-photon absorption at 4 μm. $CdGeAs_2$ has crystal growth problems. GaAs is not phase-matchable. Both $ZnGeP_2$ and $AgGaSe_2$ have been used successfully to frequency double CO_2 laser output, and $AgGaSe_2$ has been operated as an optical parametric oscillator (OPO).

Thallium arsenic selenide (Tl_3AsSe_3 or TAS) is a member of the ternary chalcogenide salt compounds with space group symmetry R3m. It is a negative uniaxial crystal and is attractive for non-linear frequency conversion because of its wide transparency range (1.3-17 μm), relatively large non-linear coefficient (similar to that of $AgGaSe_3$), fairly high damage threshold (1.7

J/cm^2) and it has been grown to large sizes (2x2x10 cm^3). Its refractive index data is well known[1] and has produced calculated phase-matched angles which are in good agreement with experiment.

Since its synthesis in 1972[2], the optical quality of TAS has improved considerably. Recent measurements of absorption were < 1%/ cm at 10 μm. In the present work, TAS was used to frequency double a CO_2 laser output with high efficiency and for the first time has also converted the CO_2 fundamental into its third, fourth and fifth harmonic.

2. Experimental.

The TAS crystals were grown, fabricated and polished at Westinghouse Research Laboratory. They were grown using the Bridgman technique and polished with diamond powder. As shown in Fig. 1, the entire crystal was mounted in a hermetically sealed aluminum cylinder. Due to the high index of refraction of TAS (∿ 3.3), the end surfaces had to be AR-coated. For the crystals TAS-1 and TAS-2, the AR-coatings were designed at 9.6 and 4.8 μm and for TAS-3, 4.8 and 2.4 μm. Unfortunately, these coatings were hygroscopic and ZnSe windows with non-hygroscopic AR coatings were used to protect the end surfaces. To facilitate angle-tuning of the crystal, the TAS crystals TAS-1 and TAS-2 were grown with the angle between the optic axis and the boule axis at 19°, and in TAS-3, at 24°. Typical dimensions of the crystals used in this work were 2.5 cm in diameter and 6 cm in length.

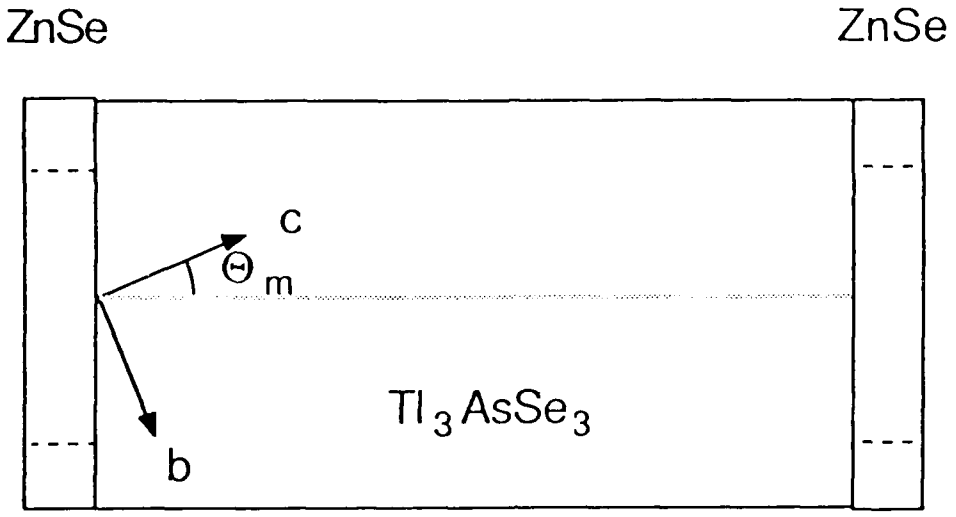

Fig. 1 -- Schematic diagram of the housing assembly for TAS. The crystal is cut at a phase match angle Θ_m for generation of the desired harmonic. The surfaces of the ZnSe windows and the ends of the crystal are AR-coated at the design wavelengths.

The pump laser used in all of the conversion experiments is a pulsed double-module Lumonics 822HP CO_2 laser. It was operated at 0.5 Hz in the TEM_{00} mode on the 9 μm P(20) transition and produced ∿ 300 mJ of linearly polarized output in a ∿ 70 ns FWHM pulse. The energies of the laser fundamental and lower harmonics were measured on a Gentec ED-500 pyroelectric detector while a Gentec ED-200 detector was used to record the fourth and fifth harmonic energies.

Frequency conversion was achieved under Type I conditions and Figs. 2-5 show schematic diagrams of the apparatus used in generating the various harmonics. The even harmonics were produced by second harmonic generation and the odd harmonics, by sum frequency conversion.

3. Results.

Fig. 6 is a graph of the second harmonic conversion efficiency with respect to the CO_2 laser fluence. Just before the onset of damage, an overall conversion efficiency of ∿28% (uncorrected for depletion) from the fundamental was measured at an incident fluence of ∿700 mJ/cm^2. This value is one of the highest second harmonic conversions of the CO_2 fundamental reported to date. It is important to note that the total energy was measured in all cases. A log-log plot of the second harmonic energy with respect to the fundamental energy is shown in Fig. 7. A least-squares-fit through the data produced a slope of ∿2.0 in excellent agreement with theory.

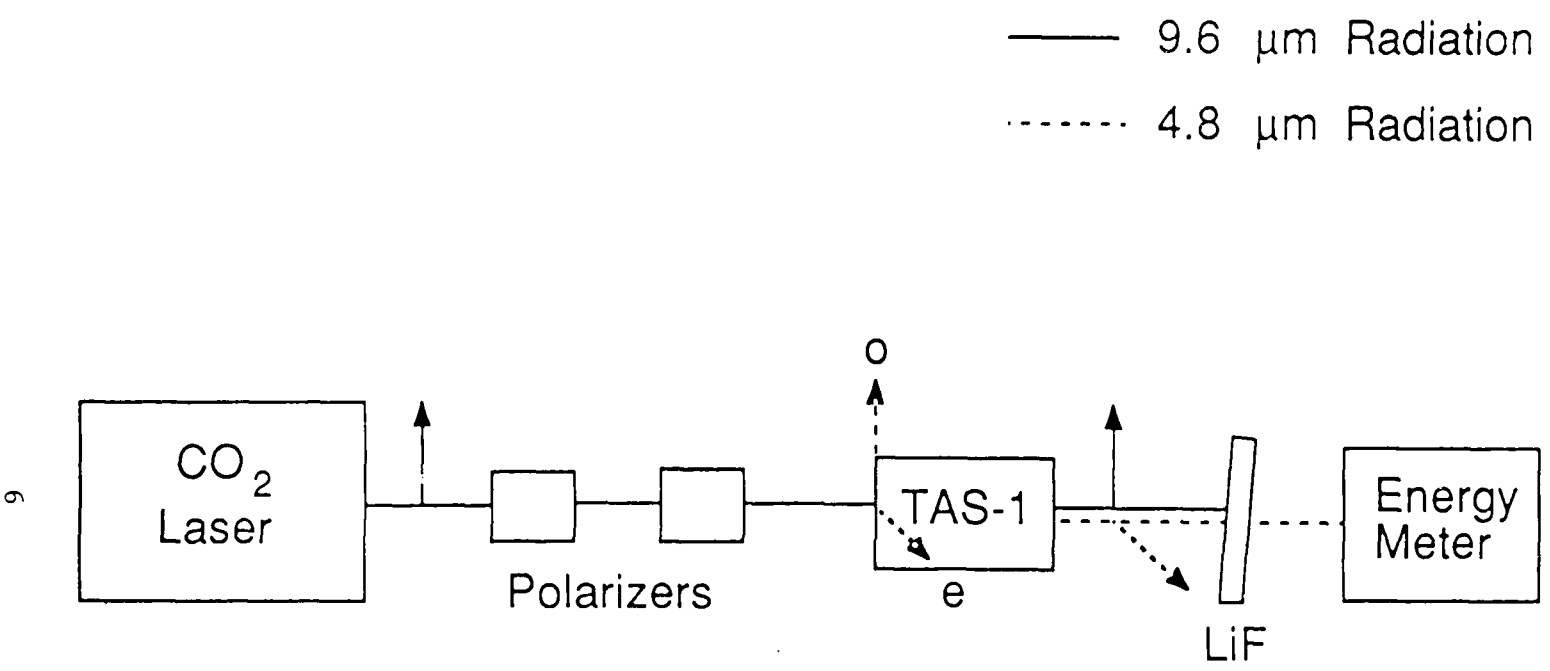

Fig. 2 -- Schematic diagram of the apparatus used for second harmonic generation (SHG). The polarizers are used to attenuate the 9.6 μm pump beam. The LiF filter is 93% transmitting at 4.8 μm. The arrowed lines indicate the polarization of the various harmonics.

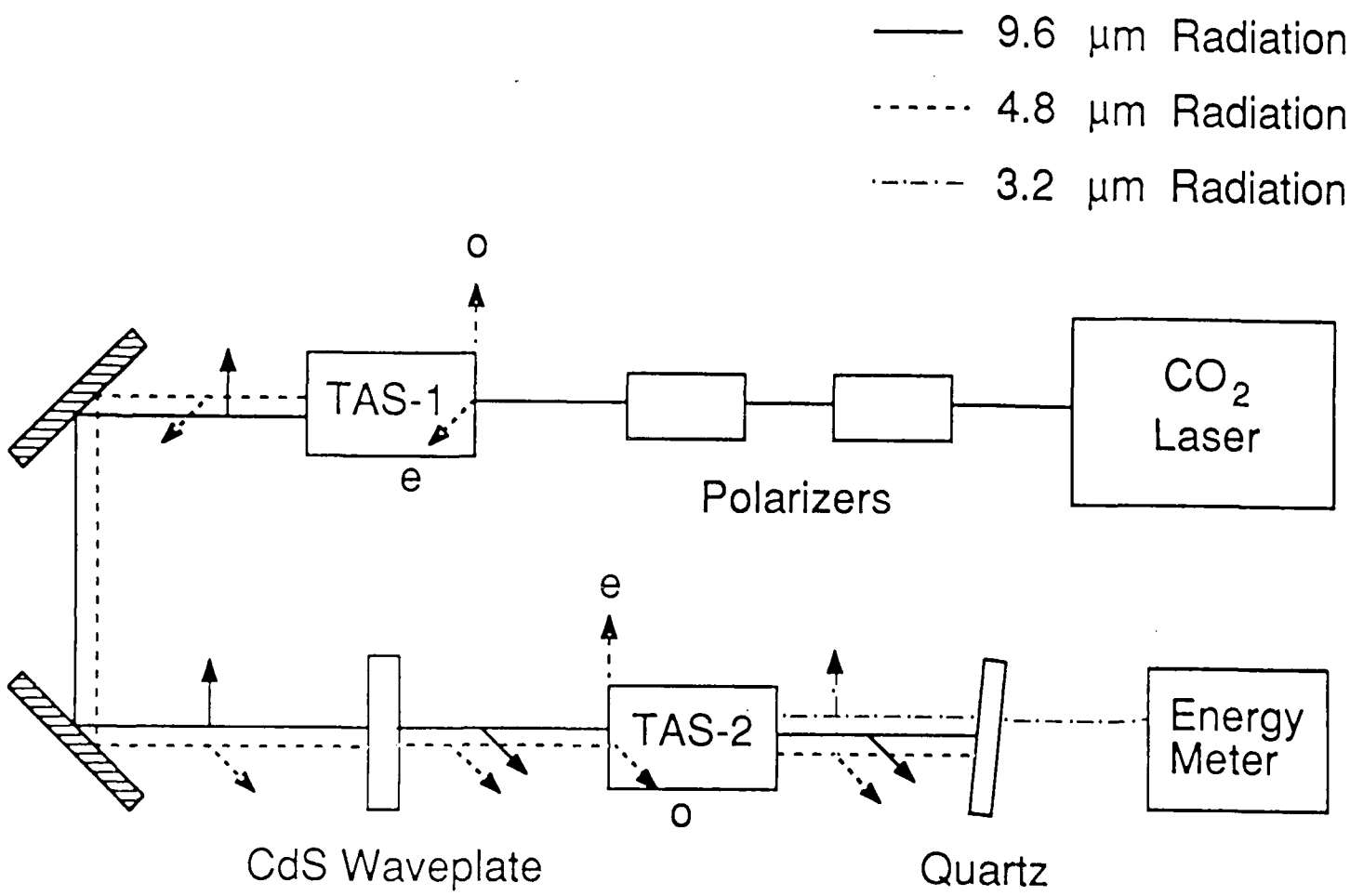

Fig. 3 -- Schematic diagram of the apparatus used for frequency tripling. The CdS waveplate is 7/2λ at 9.6 μm, 8λ at 4.8 μm and AR-coated at both wavelengths. The quartz filter is 83% transmitting at 3.2 μm. Coating losses of TAS–2 and its windows result in a crystal transmission of 23% at 3.2 μm.

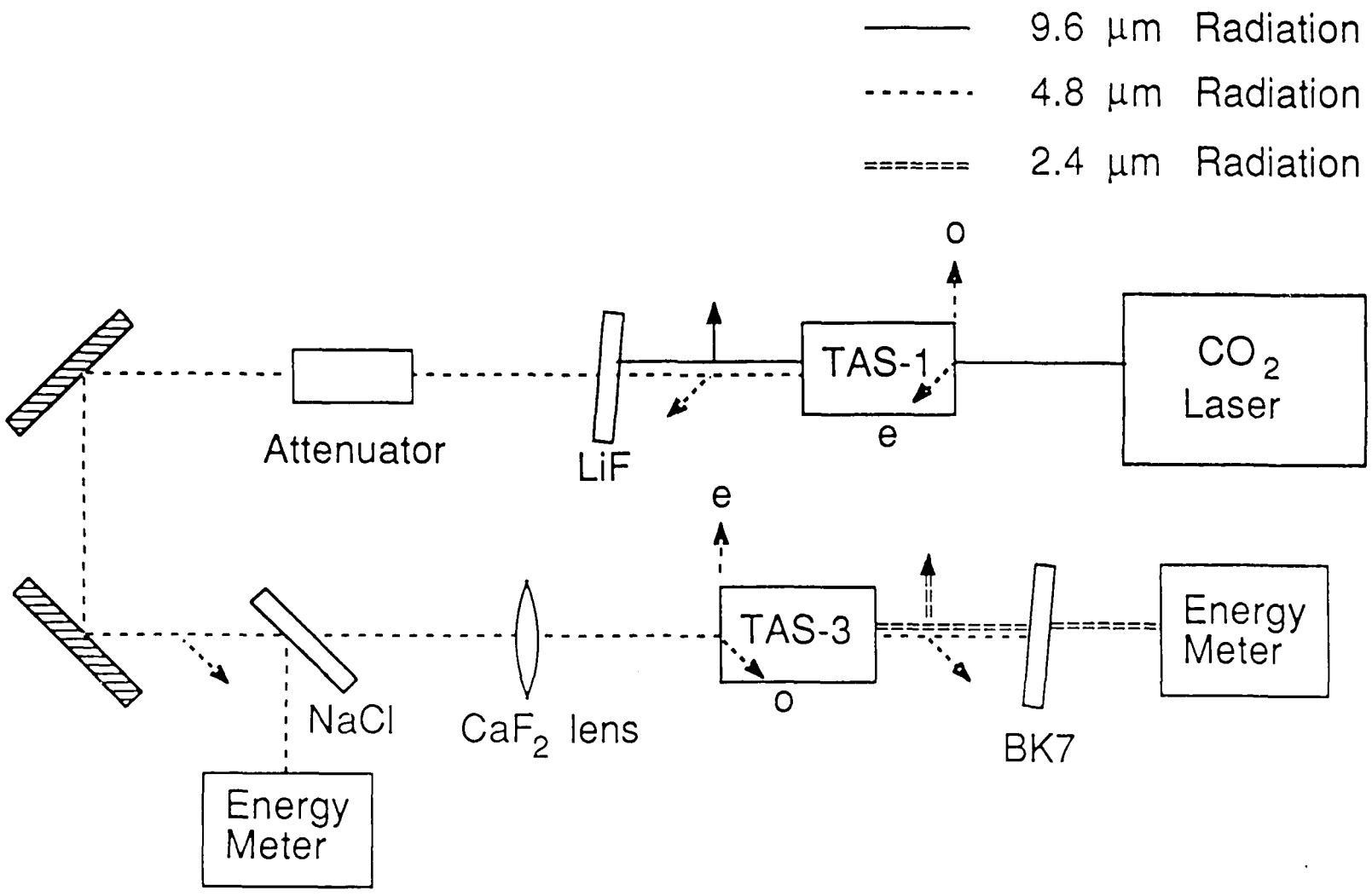

Fig. 4 -- Schematic diagram of the apparatus used in doubling the second harmonic. Coating losses of TAS-3 and its windows result in a crystal transmission of 88% and 84% at 4.8 and 2.4 μm respectively. The BK7 filter is 88% transmitting at 2.4 μm.

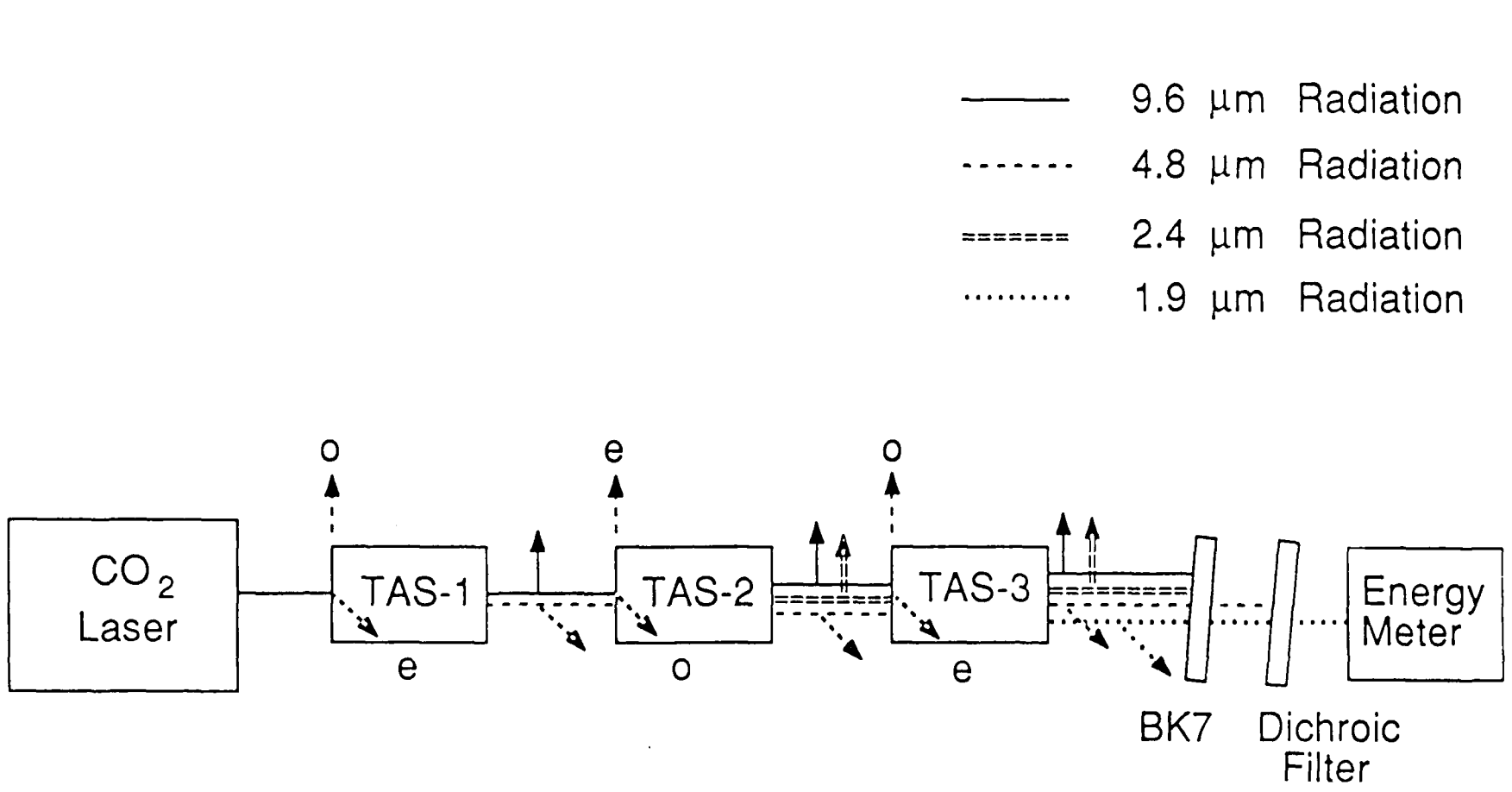

Fig. 5 -- Schematic diagram of the apparatus used in generating the fifth harmonic. Due to coating losses, the crystals TAS-2 is 30% transmitting at 2.4 μm and TAS-3 is 35% transmitting at 1.9 μm. The transmission of the BK7 and dichroic filters at 1.9 μm are 92% and 67% respectively.

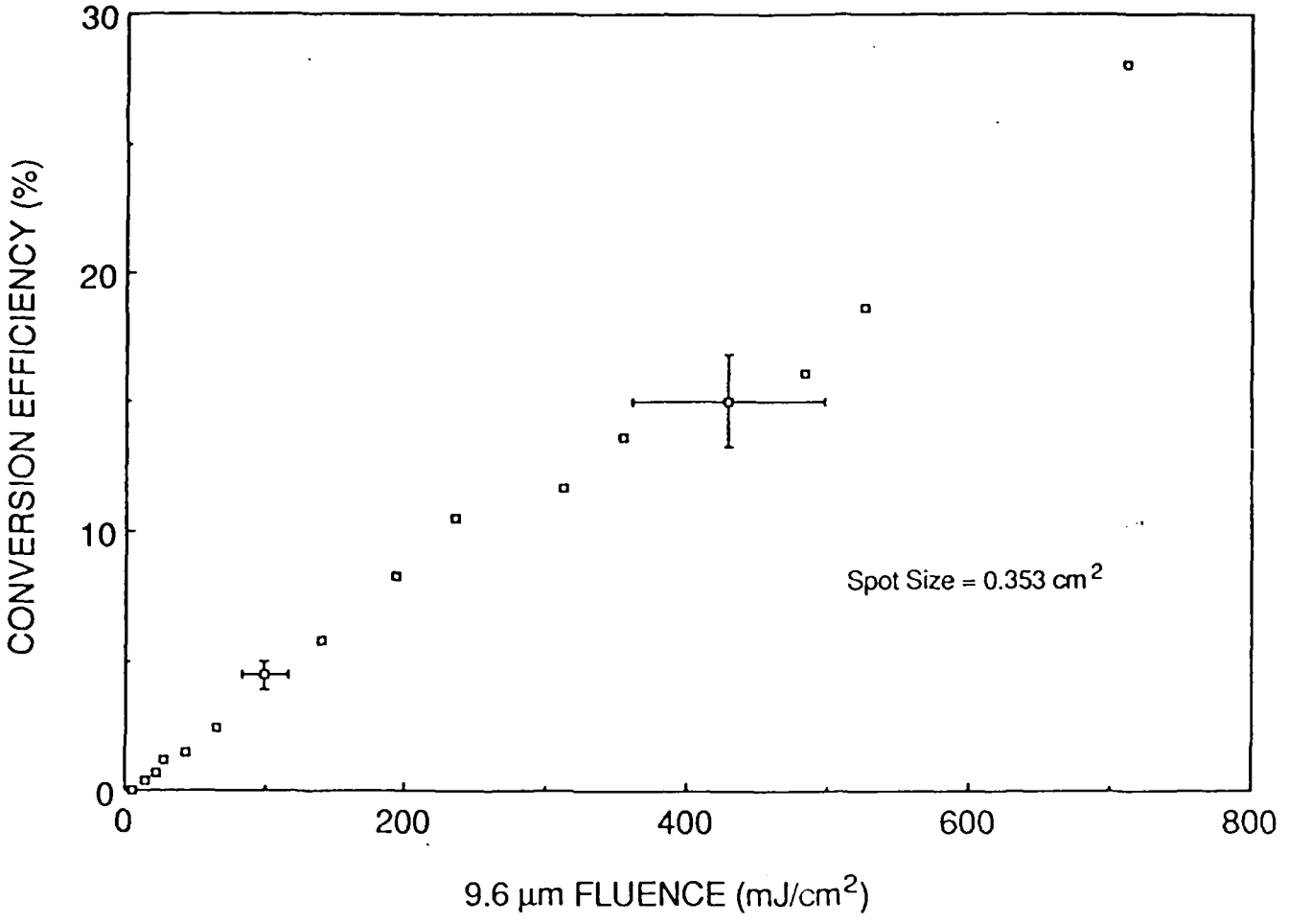

Fig. 6 -- Variation of the second harmonic energy conversion efficiency as a function of 9.6 μm pump fluence. The spot size area contains ~50% of the total 9.6 μm energy.

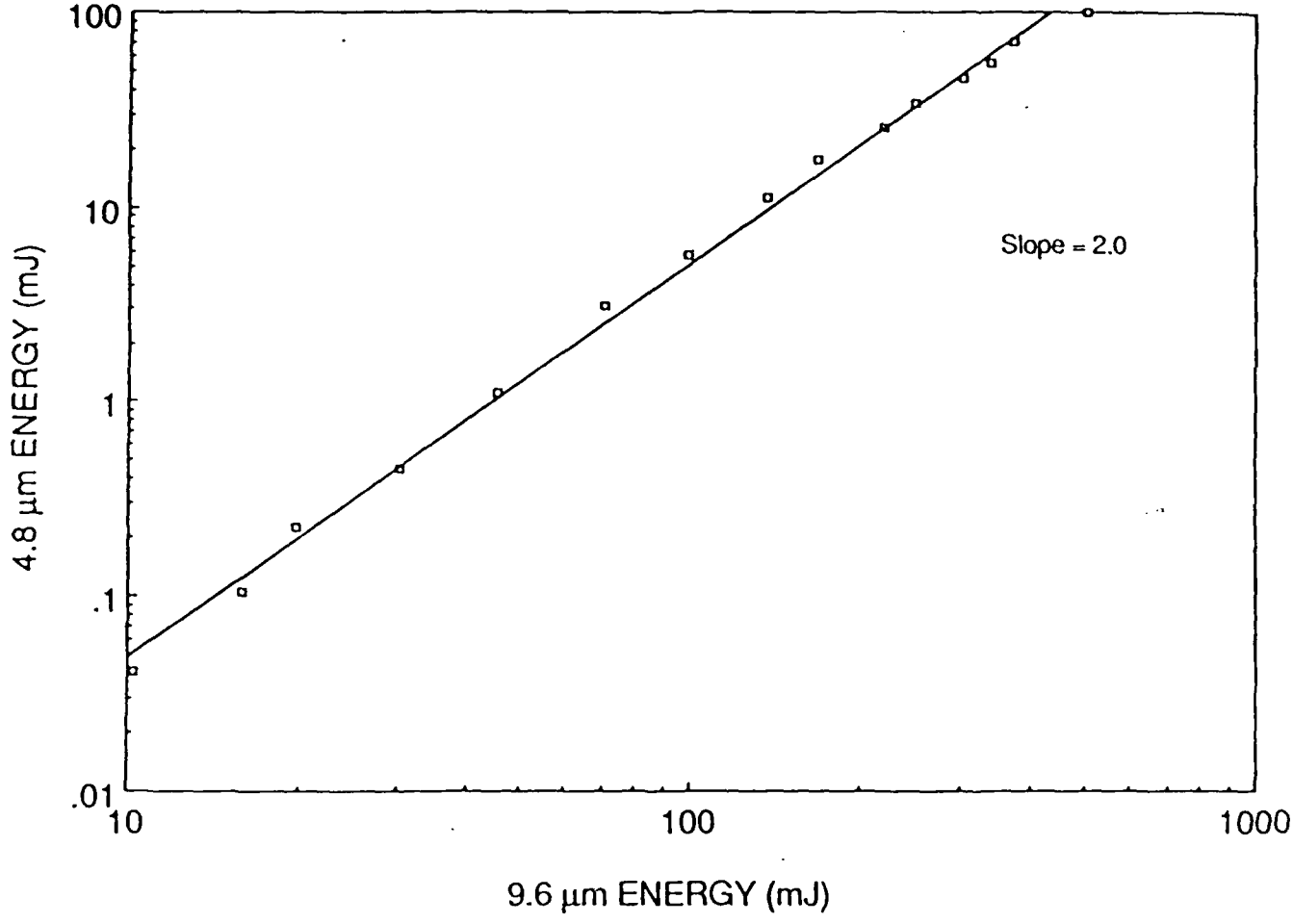

Fig. 7 -- Variation of the 4.8 µm energy as a function of 9.6 µm pump energy.

The third harmonic was generated by sum frequency conversion in a second crystal tuned close to the phase match angle of $\sim 21^{o}$. In order to perform Type I tripling, the CdS waveplate rotated the 9.6 μm polarization by 90^{o} while leaving the 4.8 μm polarization essentially unchanged. Fig. 8 is a graph of the third harmonic energy conversion efficiency with respect to the pump fluence. At an incident fluence of $\sim$ 370 mJ/cm^2, a maximum external (internal) conversion of 5.5% ($\sim$12%) was measured. A log-log plot of the third harmonic energy with that of the fundamental is shown in Fig. 9. A least-squares-fit through the data produced a slope of $\sim$2.5 which is less than the anticipated value of 3. This discrepancy is probably due to crystal inhomogeneity and poor 4.8 μm beam quality.

The fourth harmonic was generated by doubling the second harmonic in another TAS crystal which was tuned close to the phase match angle of $\sim 27^{o}$. Because in preliminary experiments, no evidence of damage was observed in TAS-3 with the raw 4.8 μm output from TAS-1, a CaF_2 lens (50 cm f.l.) was placed $\sim$ 26 cm from TAS-3 to obtain a higher 4.8 μm pump fluence. A plot of the fourth harmonic conversion with respect to the second harmonic fluence is shown in Fig. 10. At an incident fluence of $\sim$170 mJ/Cm^2, an external (internal) conversion efficiency of 26% (30%) was measured. It is interesting to note that since the second harmonic conversion efficiency varies a ω^2, the same efficiency can be achieved in the fourth harmonic case as in the second harmonic case but with one-quarter the pump fluence. Therefore, high conversion efficiencies are easier to achieve with shorter pump wavelengths. A log-log plot of the fourth harmonic energy with that of the second is shown in Fig. 11. A least-squares-fit

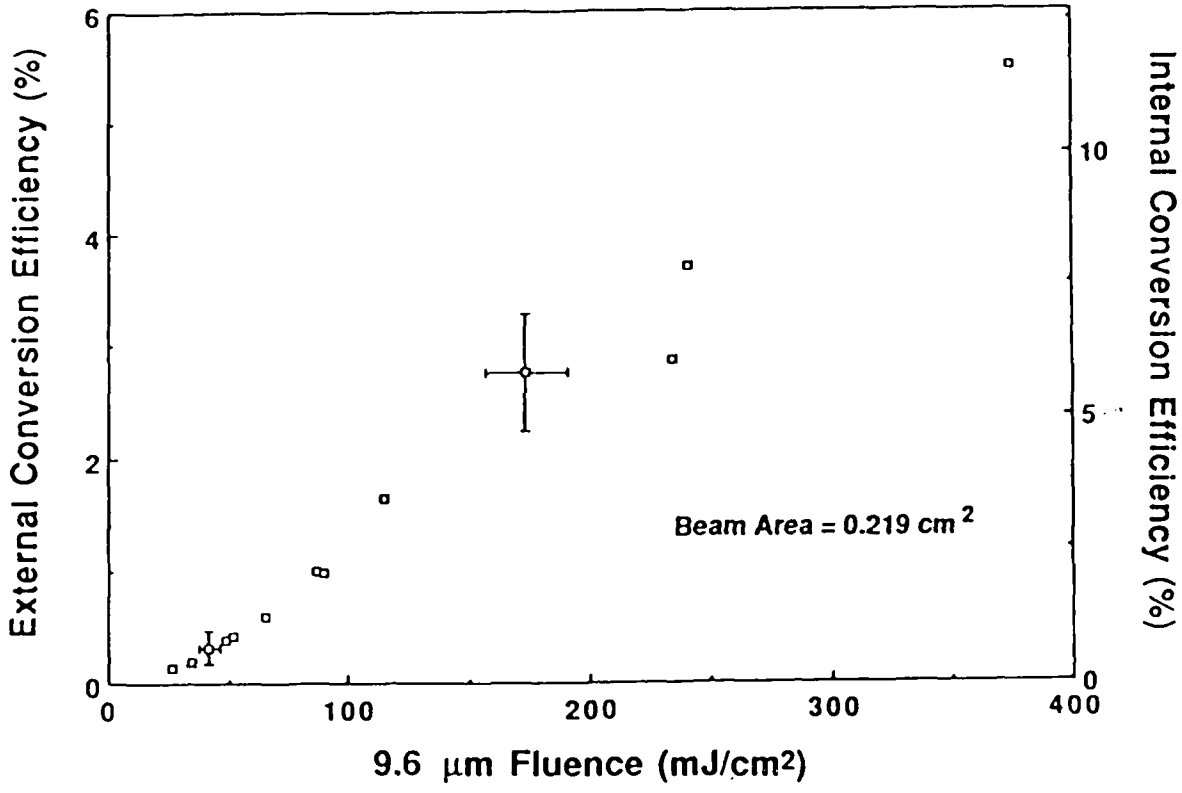

Fig. 8 -- Variation of the third harmonic energy conversion efficiency (with respect to the fundamental) as a function of 9.6 μm fluence. The external efficiency corrects for losses at the quartz filter whereas the internal efficiency includes the coating losses of TAS-2 at 3.2 μm. The spot size area contains ~50.% of the total 9.6 μm energy.

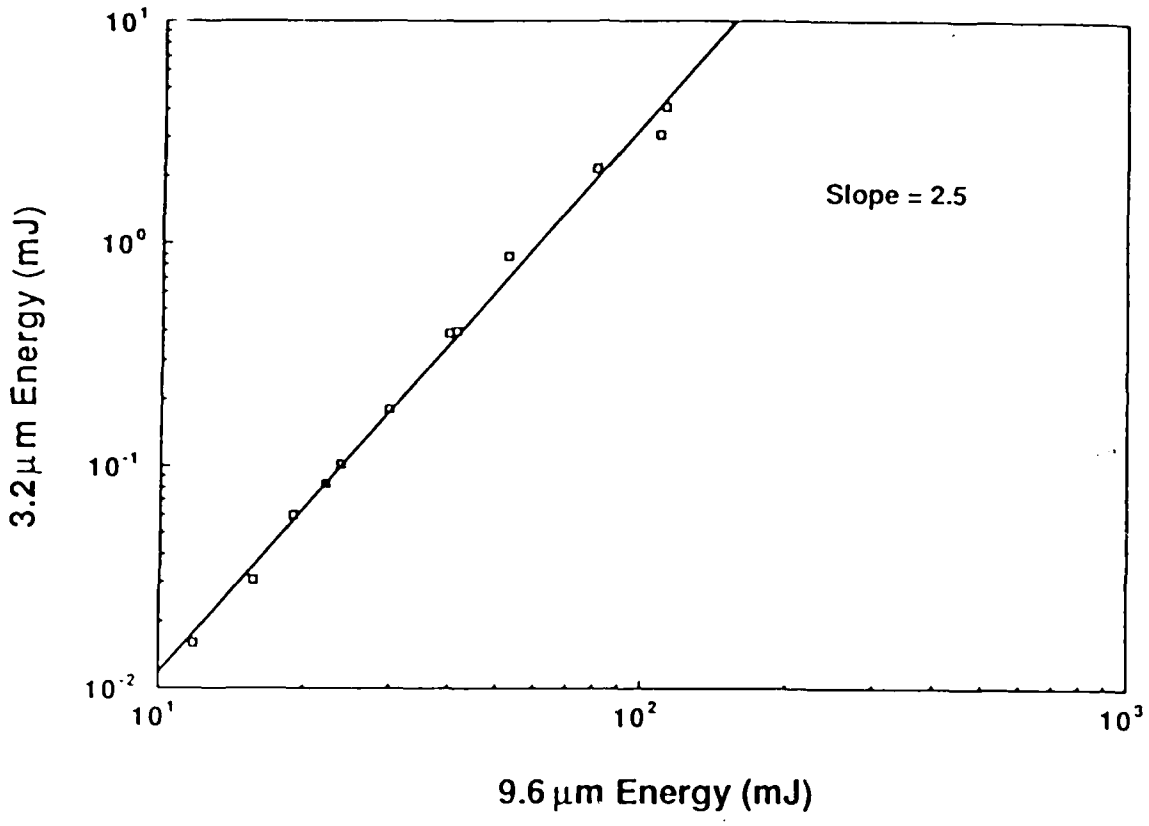

Fig. 9 -- Variation of the third harmonic energy as a function of the 9.6 μm pump energy.

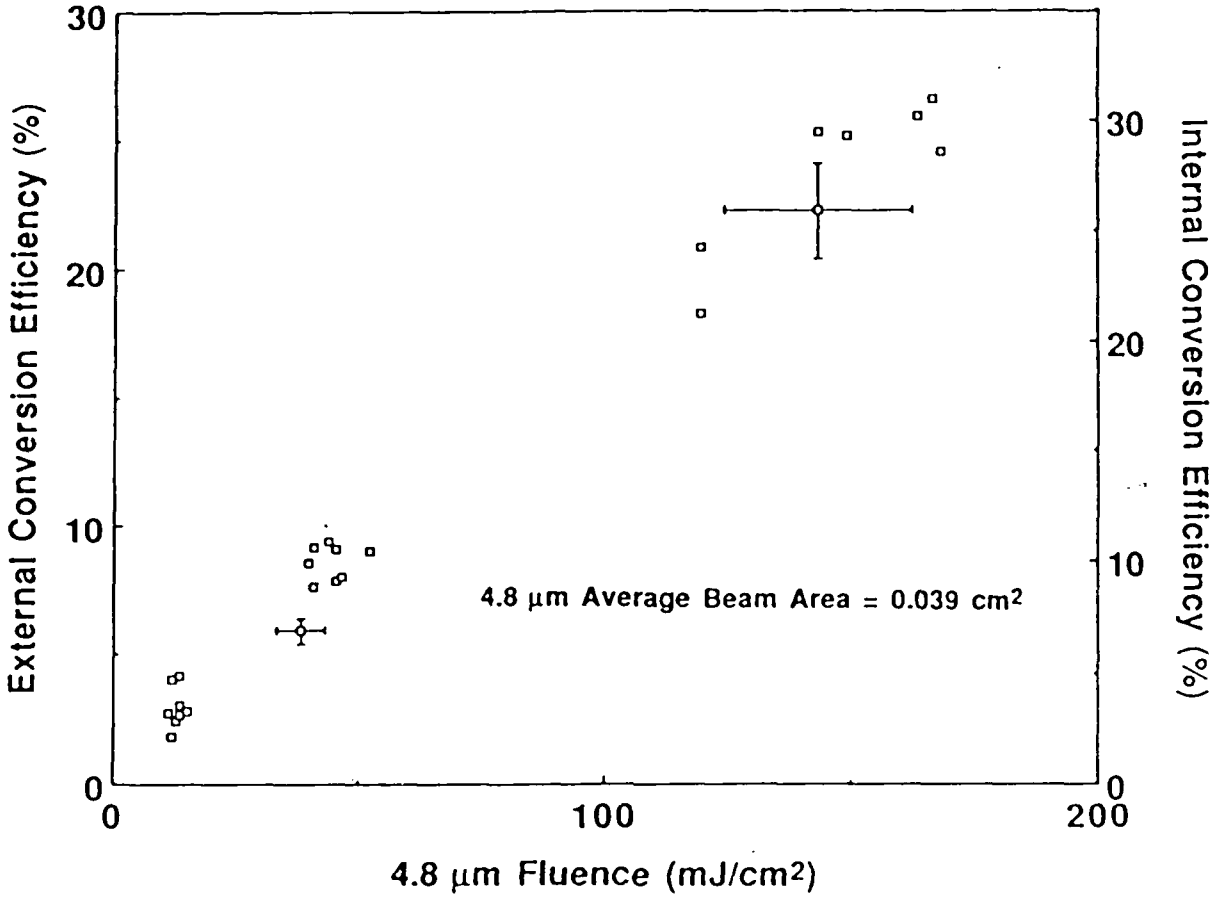

Fig. 10 -- Variation of the fourth harmonic energy conversion efficiency (with respect to the second harmonic) as a function of 4.8 μm pump fluence. The external efficiency corrects for losses at the BK7 filter and the internal efficiency includes the coating losses of TAS-3 at 4.8 μm and 2.4 μm. The spot size area contains 50% of the total 4.8 μm energy and is measured at the center of the crystal.

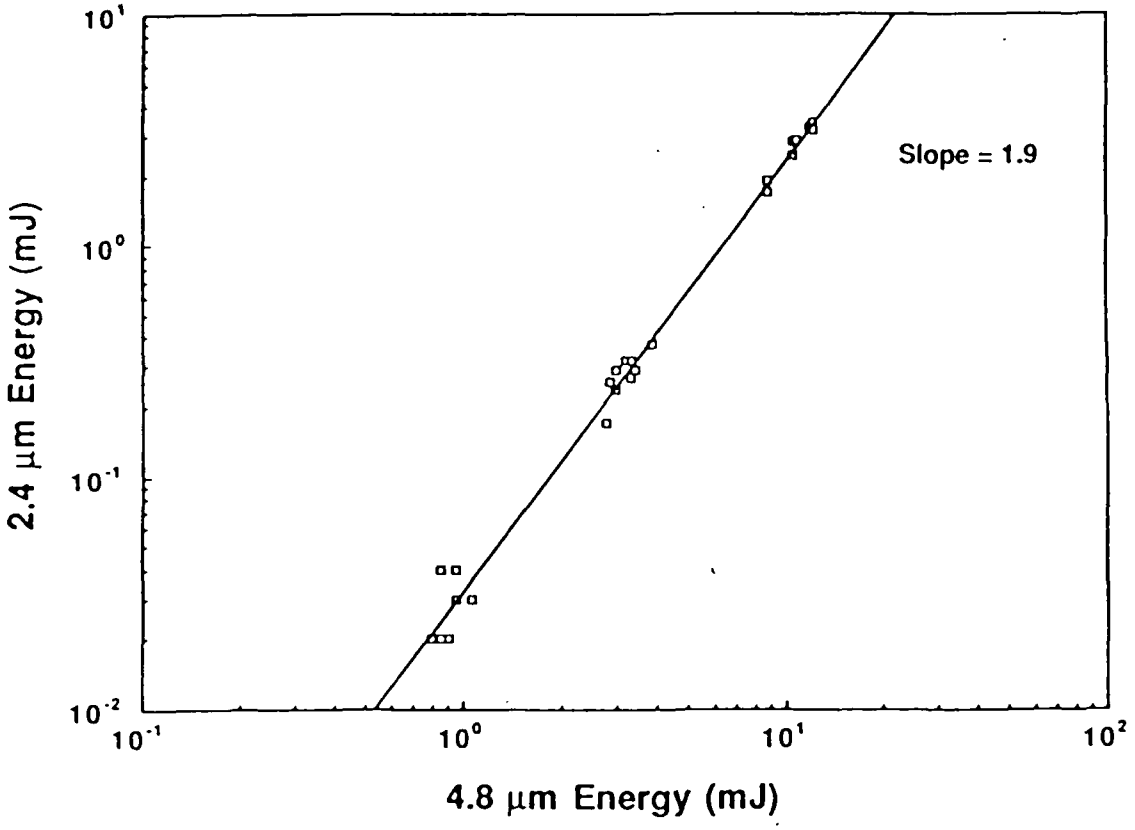

Fig. 11 -- Variation of 2.4 µm energy as a function of 4.8 µm energy.

through the data results in a slope of 1.9, in very good agreement with theory.

Encouraged by the high fourth harmonic conversions, it was decided to use the same crystal (TAS-3) to produce the fifth harmonic by summing the fundamental and the fourth harmonic. Under Type I conditions and at 9.6 μm and 2.4 μm fluences of 180 and 12 mJ/cm^2 respectively, ∿ 400 μJ of 1.9 μm output was obtained, correcting for losses only at the filters. If the losses at the AR coatings are included, an internal conversion efficiency of 45% from the fourth harmonic or 0.5% from the fundamental was achieved.

4. Conclusions.

In this work, TAS has been used to convert the 9.6 μm CO_2-laser fundamental to its second harmonic with high efficiency and for the first time, to its third, fourth and fifth harmonic. A summary of the measured external and internal conversion efficiencies is shown in Table 1. Although the generated harmonics do not completely cover the near- to mid-IR region, it is important to note that the CO_2 laser itself is tunable between 9-11 μm and therefore there is a band of tunability associated with each harmonic. Attempts to build a TAS-based OPO were unsuccessful, although evidence of optical parametric amplification of ∿ 1%/pass were observed.

In summary, this work has demonstrated TAS to be a promising material for CO_2 frequency conversion and a potential source of tunable radiation in the IR. The measured harmonic conversion efficiencies are encouraging and with further improvements in

Table 1 -- Summary of measured external and internal energy conversion efficiencies with respect to the 9.6 μm CO_2-fundamental. The pump fluences represent the actual energy deposited into the crystal.

Harmonic	External	Internal	E_ω/A (int.)
2ω	28 %	28 %	660 mJ/cm^2
3ω	5.5	12	370
4ω	2.8	3.3	($E_{2\omega}/A$=170)
5ω	0.3	0.5	180

optical quality and AR coating of the crystals, even higher conversions are anticipated.

III. Argon/Xenon Laser.

1. Background.

The Ar/Xe laser, operating on the 5d-6p Xe transitions, has been demonstrated to have high efficiency (3-5%) and specific output energy (to 6 J/l) when pumped in an e-beam sustained discharge[3]. When operated in an electron-beam pre-ionized mode, however, a lower efficiency (1.3%) and specific energy (.67 J/l) are reported[4]. With UV pre-ionization and a fast transverse discharge, an efficiency similar to the latter (1.4%), but at much lower energy loading and, therefore, specific output energy (0.1 J/l) has been reported[5]. All of these experiments used similar power loadings on the gas, but the last work had very short discharge pulses compared to the electron beam results, which limited the specific energy, while the UV pre-ionization also limited the pressure to 1.4 atmospheres. These results, however, can be compared to the rare gas halide lasers in its high pressure operation, potential efficiency and specific energy, and through similarities in the kinetics processes involved. There are two obvious major differences. First, the lack of the halogen gas results in the significant advantages of long pulse operation, as there is no fuel "burn-up", and long gas lifetime and simple high repetition rate operation. Second, the laser operates on atomic, not molecular transitions, so that the linewidth can be narrow, the gain can be high and the lower laser

levels exist and participate in the kinetics. The laser is also, apparently, limited to a much lower pump intensity than the excimers, but the long pulse lengths which have been achieved with the electron beam sustained or pre-ionized systems allow similarly high specific energies.

2. Energy Levels and Kinetics.

While the laser has been observed to operate on six transitions in the 5d-6p manifold, the dominant line is the $5d[3/2]^{o}_{1}$-- $6p[5/2]_2$ transition, at 1.73 μ. The most important kinetics processes populating the upper levels can be listed as:

$$Ar^+ + 2\ Ar \rightarrow Ar_2^+ + Ar \quad Ar_2^+ + Xe \rightarrow Xe^+ + 2\ Ar \qquad (1)$$

$$Ar_2^+ + Xe \rightarrow ArXe^+ + ArXe^+ + 2\ Ar \rightarrow ArXe+ + Ar \qquad (2)$$

$$ArXe^+ + e \rightarrow ArXe^{**} \rightarrow Xe^{**}(5d) + Ar \qquad (3)$$

The high efficiency observed in Ref. 3 was accounted for by postulating "recirculated pumping" from the Xe 6s metastable level, followed by ionization and subsequent recombination through equation (3). This channel is certainly desirable because of the much higher quantum efficiency possible due to ionization from the high lying metastable level rather than direct pumping of the upper level or ionization from the ground state, and may be operable in the e-beam or uv preionized discharge lasers, since the metastable lifetime is estimated to be about 0.5 μ s. An examination of the rates indicates that high E/P is necessary for populating the metastable levels, while the

recombination process operates at low E/P. In the e-beam sustained work, the metastable population was said to be created by the high energy e-beam itself, while the low energy electrons of the discharge were responsible for the recirculation pumping. Ringing of the preionized discharge, so that the E/P alternated between high and low values, was discussed in Ref. 4.

3. Experimental.

Experiments with electron-beam pumping, electron-beam sustained discharge pumping, and x-ray preionized discharge pumping were performed in order to investigate the mechanisms and potential of this laser system under these different conditions. The electron beam apparatus is a small device, operable at 175-250 kV gun voltage, with a current through the 2 x 40 cm foil window of 1 to 5 A /cm^2 and pulse lengths of 0.6 to 1.2 μs. The laser chamber has an electrode spacing of 3 cm, and an extractable volume of 125 cm^2. When operated with electron-beam pumping alone, a maximum output of 90 mJ was observed, at 250 kV gun potential with a 1 mil Ti foil window, using a mixture of 1% xenon in 4 atmospheres of argon. The output energy observed as a function of gun voltage and pressure reflects optimization of energy deposition into the laser volume. Based on our calculation of energy deposition, we estimate the efficiency to be 1%. The results are comparable to those achieved in the literature when the relatively short pulse length of our device is considered.

For operation in the e-beam sustained mode, a simple switchand capacitor circuit was used. A thicker, 1.5 mil foil

and cathode grid used to prolong foil lifetime resulted in much lower laser output from the e-beam alone. At the maximum gun voltage, 12 mJ was observed from a 2.3% mixture at 3 atmospheres pressure and application of the discharge resulted in a maximum total output of 48 mJ, an enhancement factor of 4. An enhancement factor of 11 was observed when the e-beam contribution was reduced to 3 mJ and the discharge circuit improved. In order to investigate the high specific energy, high efficiency regime of operation used in Ref. 3, modification of the e-beam to produce longer pulses and higher currents is necessary.

Interesting line competition effects have been observed. The laser begins on either the 2.63 μm or 2.65 μm line (our filter cannot distinguish between them). Output then switches to the 1.73 μm line, which dominates the output. That line also terminates, to be followed by lasing again at 2.6 μm. While the initial behavior can be explained on the basis of gain and degeneracy effects, the later behavior cannot, implying interesting upper and lower level population dynamics.

In using a computer code to model this laser, the critical recombination pump rate (3) is not known and must be estimated. However, even with this approximation we have seen reasonable agreement in discharge voltage, current and laser pulse shape.

4. Conclusions.

The results reported above include a specific output energy of 0.75 J/l using the electron beam alone, enhancements of up to a factor of 10 using electron beam sustained discharge pumping,

and the first reported lasing from an x-ray preionized discharge, using a device with a 5 cm electrode gap. Line competition has also been observed.

These results are far from optimal. Significant increases in laser output and efficiency are expected to result from modifications to the electron beam and preionized systems. In order to investigate the kinetics of the laser, diagnostics to measure the gain and important populations should be implemented.

IV. References.

1. M.D Ewbank et al., J. Appl. Phys., 51, 3848 (1980).

2. J.D. Feichntner and G.W. Roland, Appl. Opt., 11, 993 (1972).

3. N.G. Basov et al., IEEE J. Quantum Electron., QE-21, 1756, (1985).

4. S.A. Lawton et al., J. Appl. Phys. 50, 3888, (1979).

5. F.S. Collier et al., IEEE J. Quantum Electron., QE-19, 1129, (1983).

END

DATE

FILMED

MARCH

1988

DTIC